Supplementary Information

- **Supplementary Fig. 1. Proteins and pathogenetic pathways for SRNS genes and data on pedigree structure, Sanger sequencing, renal ultrasound and histology in patients with *GAPVD1* and *ANKFY1* mutations.**
- **Supplementary Fig. 2. Homozygosity Mapping.**
- **Supplementary Fig. 3. Subcellular localization of GFP-tagged *GAPVD1* cDNA overexpression constructs in a human podocyte cell line.**
- **Supplementary Fig. 4. Subcellular localization of *ANKFY1* constructs in endosomes, and co-localization with GAPVD1.**
- **Supplementary Fig. 5. GAPVD1 interacts with ANKFY1 and nephrin.**
- **Supplementary Fig. 6. RAB5 activity assay and lack of an effect of *GAPVD1* overexpression on tracer endocytosis in human podocyte cell line.**
- **Supplementary Fig. 7. Characterization of stable shRNA lines used to measure podocyte migration rate for GAPVD1 (see Fig. 5A).**
- **Supplementary Fig. 8. Characterization of stable shRNA lines used to measure podocyte migration rate for *ANKFY1* (see Fig. 5B).**
- **Supplementary Fig. 9. Phenotype of a second *Gapvd1-RNAi,* and qPCR analysis.**
- **Supplementary Fig. 10. Hypothetical working model for GAPVD1 and ANKFY1 loss-of-function in podocytes.**
- **Supplementary Table 1: Primer sequences**

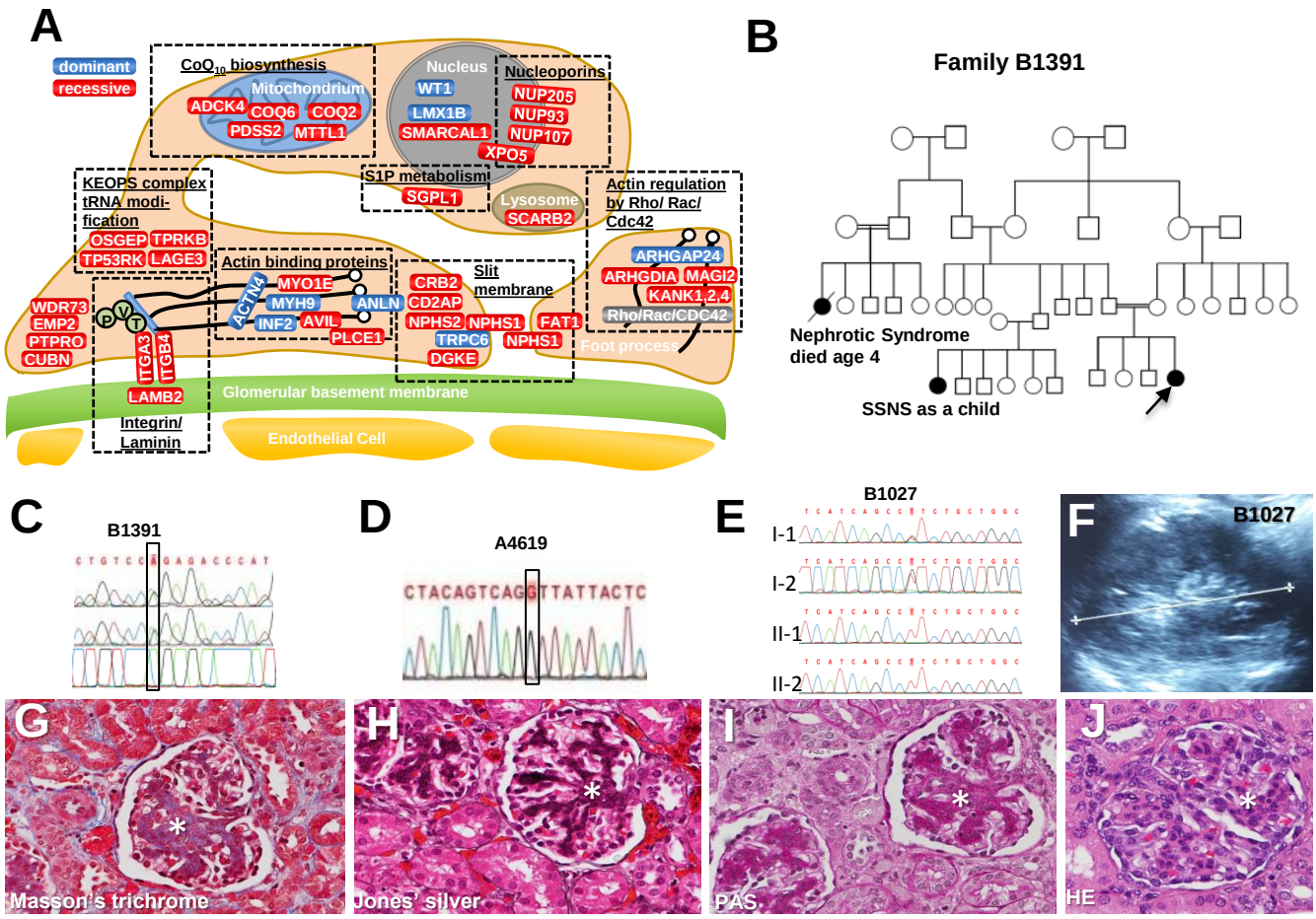

Supplementary Fig. 1. Proteins and pathogenetic pathways for SRNS genes and data on pedigree structure, Sanger sequencing, renal ultrasound and histology in patients with *GAPVD1* and *ANKFY1* mutations.

(A) The schematic depicts a simplified podocyte with the proteins involved in single-gene causes of SRNS. Proteins are shown in red when causative mutations have been described as recessive and blue for dominant mutations. These SRNS-related proteins are part of protein–protein interaction complexes that participate in defined structural components or signaling pathways of podocyte function (black frames). These genes thus delineate pathogenetic pathways of SRNS.

(B) Pedigree of family B1391 with multiple individuals affected with nephrotic syndrome (arrow indicates proband). Further family members were unavailable for genetic analysis. Consanguinity loops are indicated by double horizontal lines. Squares denote males, circles females, filled symbols denote affected individuals.

(C-E) Sanger sequencing traces confirming the mutations and segregations for B1391 **(C)**, A4619 **(D)**, and B1027 **(E)**. DNA from the parents of A4619 were unavailable for sequencing.

(F) Renal ultrasound of B1027 reveals no significant anomalies.

(G-J) Additional images (see **Fig. 1F-H**) from renal nephrectomy of A4619 confirm mesangial hypercellularity and expansion of the extracellular matrix (asterisks).

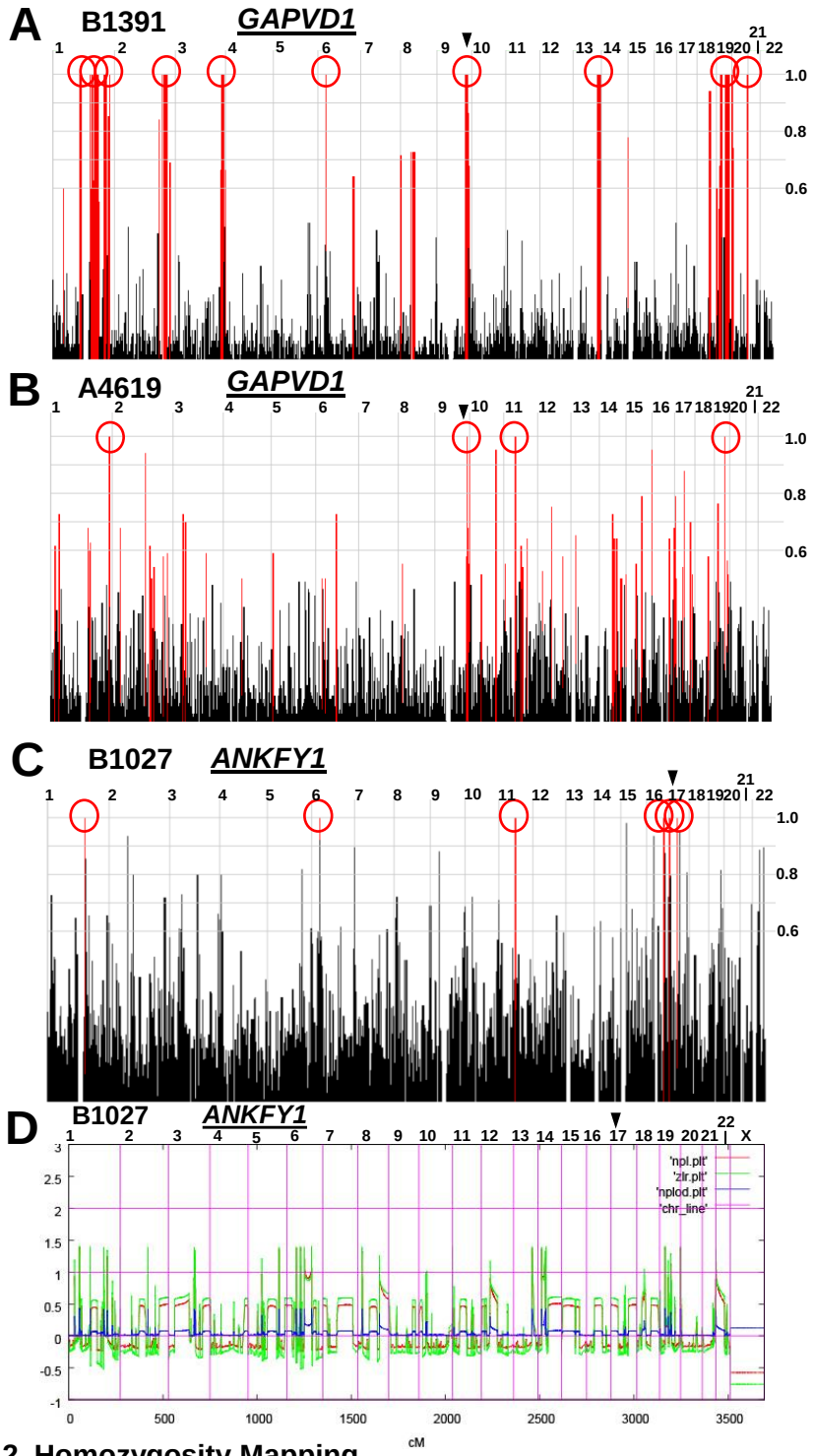

Supplementary Fig. 2. Homozygosity Mapping.

(A) Nonparametric LOD (log of the odds ratio) (NPL) score profile across the human genome in one individual with SRNS of consanguineous family B1391. Ten maximum NPL peaks (red circles) indicate candidate regions of homozygosity by descent. *GAPVD1* is positioned (arrowhead) within a peak on chromosome 9.

(B) NPL score profile for individual A4619. Six maximum NPL peaks (red circles) indicate candidate regions of homozygosity. *ANKFY1* is positioned (arrowhead) within a peak on chromosome 17.

(C) NPL score profile across the human genome of linked analysis of two siblings of distantly consanguineous family B1027. Six maximum NPL peaks (red circles) indicate candidate regions of homozygosity by descent. *ANKFY1* is positioned (arrowhead) within a peak on chromosome 17 that is shared between both siblings.

(D) Linkage analysis indicates a shared region for both siblings around the ANKFY1 locus (arrow head).

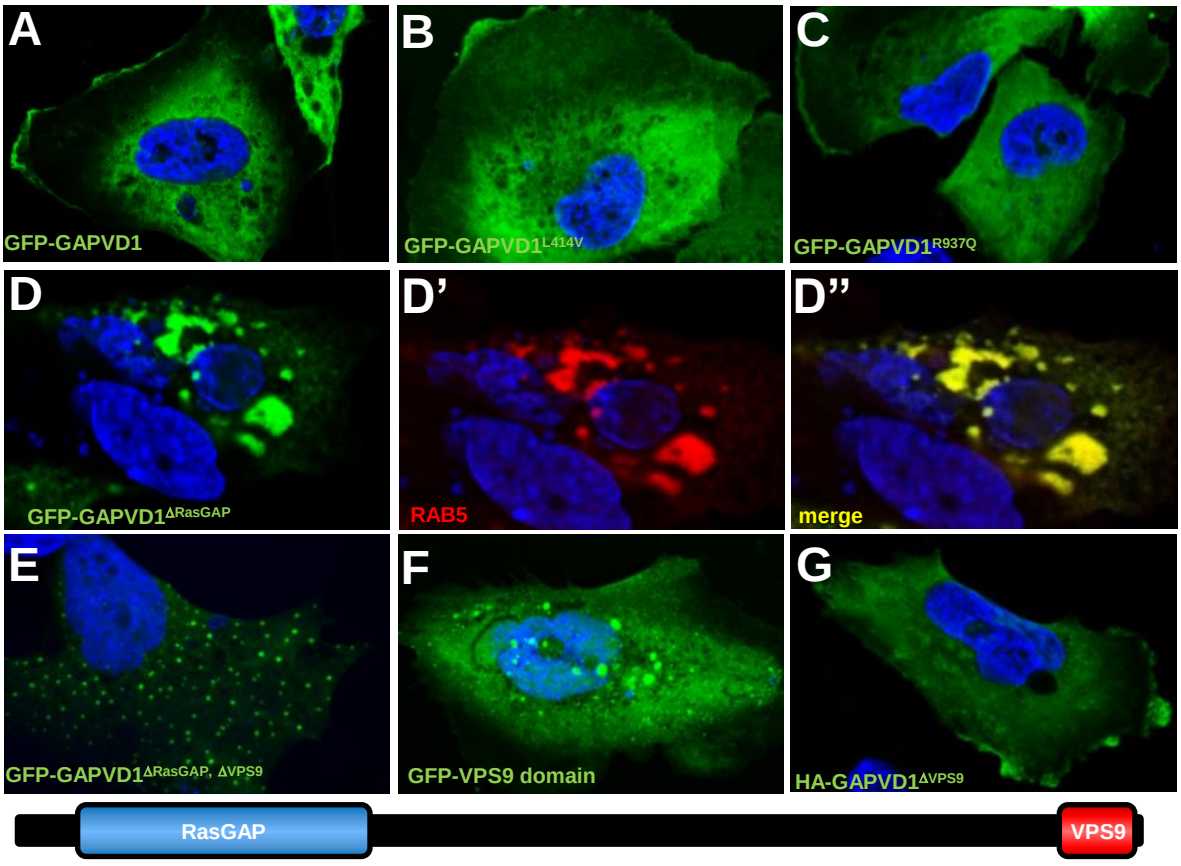

Supplementary Fig. 3. Subcellular localization of GFP-tagged *GAPVD1* cDNA overexpression constructs in a human podocyte cell line.

(A-C) Overexpressed GFP-GAPVD1 localizes to the cytosol in podocytes **(A)**. Overexpression of constructs reflecting the mutations L414V **(B)** or R937Q **(C)** does not alter subcellular localization. Weak GFP signal that may appear intranuclear most likely derives from perinuclear cytoplasm above or below.

(D-D'') A GFP-*GAPVD1*-construct that lacks the inhibitory RasGAP domain localizes to vesicles that co-stain with an anti-RAB5 antibody.

(E) Deletion of both functional domains of *GAPVD1* (ΔRasGAP, ΔVPS9, see **Fig. 3D**) results in a vesicular localization.

(F) A GAPVD1 construct that is restricted to the VPS9 domain (GFP-VPS9) localizes to vesicles.

(G) Deletion of the VPS9 domain from GAPVD1 does not alter the subcellular localization compared to wild type GFP-*GAPVD1* overexpression.

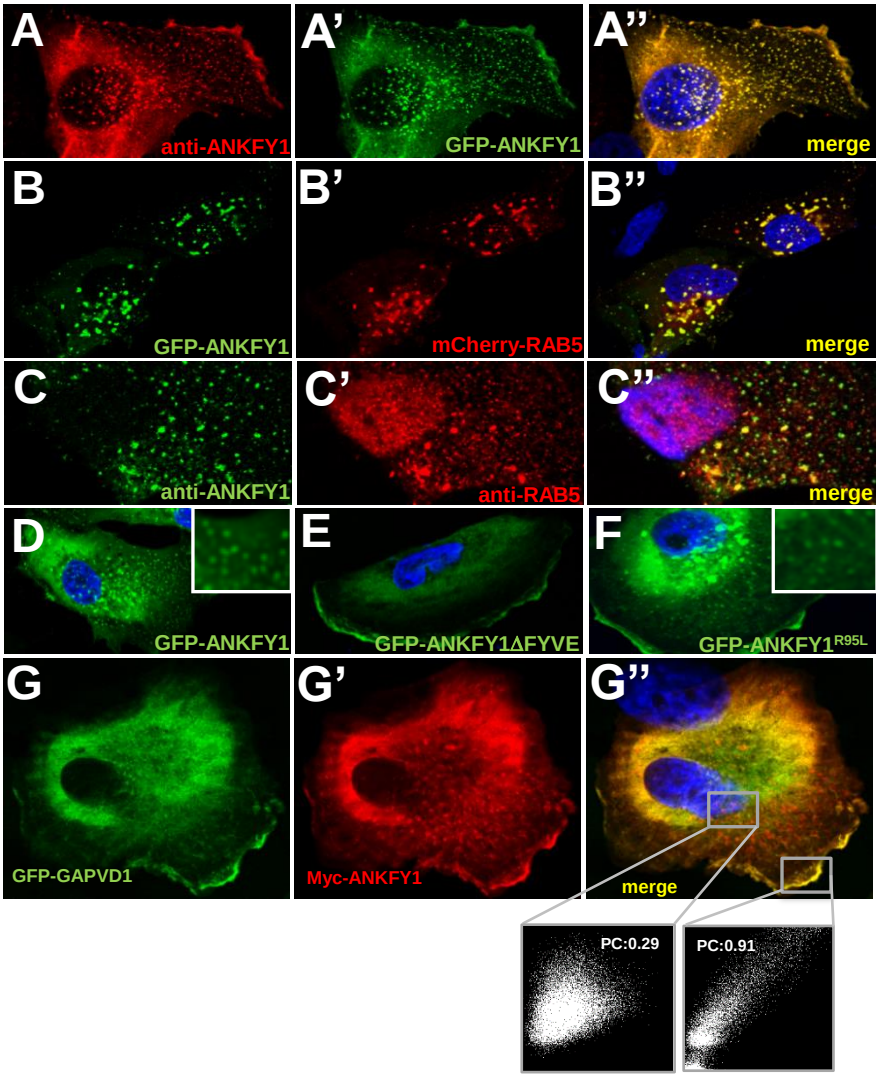

Supplementary Fig. 4. Subcellular localization of *ANKFY1* constructs in endosomes, and co-localization with GAPVD1.

(A-A'') A monoclonal mouse anti-ANKFY1 antibody detects GFP-tagged ANKFY1 overexpressed in podocytes.

(B-B'') Overexpressed GFP-tagged ANKFY1 and overexpressed mCherry-RAB5 co-localize to vesicles in podocytes.

(C-C'') Endogenous ANKFY1 partially co-localizes to vesicles with endogenous RAB5.

(D) Overexpressed GFP-tagged ANKFY1 localizes to vesicles in podocytes (inset shows detail from the same).

(E) Deletion of the FYVE domain of GFP-ANKFY1 abrogates the vesicular localization of the overexpressed protein.

(F) Overexpression of GFP-ANKFY1 reflecting the mutation Arg95Leu of an SRNS patient shows no obvious alteration of the subcellular localization.

(G-G'') GFP-GAPVD1 and Myc-ANKFY1 show partial co-localization in cultured human podocytes.

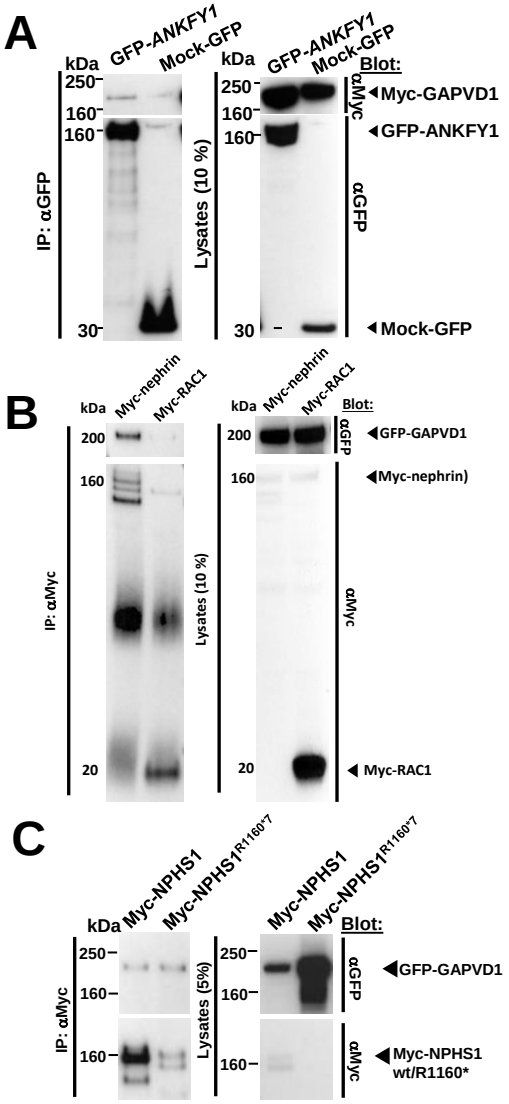

Supplementary Fig. 5. GAPVD1 interacts with ANKFY1 and nephrin.

(A) Upon overexpression and co-IP with anti-GFP antibody GFP-tagged ANKFY1, but not mock-GFP, precipitates Myc-tagged GAPVD1 in HEK293T cells.

(B) Upon overexpression and co-IP Myc-tagged NPHS1 but not Myc-tagged RAC1 precipitate GFP-tagged GAPVD1.

(C) A construct representing a mutation in patients with SRNS, which results in a premature stop and loss of the last 82 amino acids (R1160*, see **Fig. 1D**), shows interaction with GAPVD1. This suggests that the c-terminal half of the cytosolic domain of nephrin (see Fig. 3D) is not critical for interaction with GAPVD1.

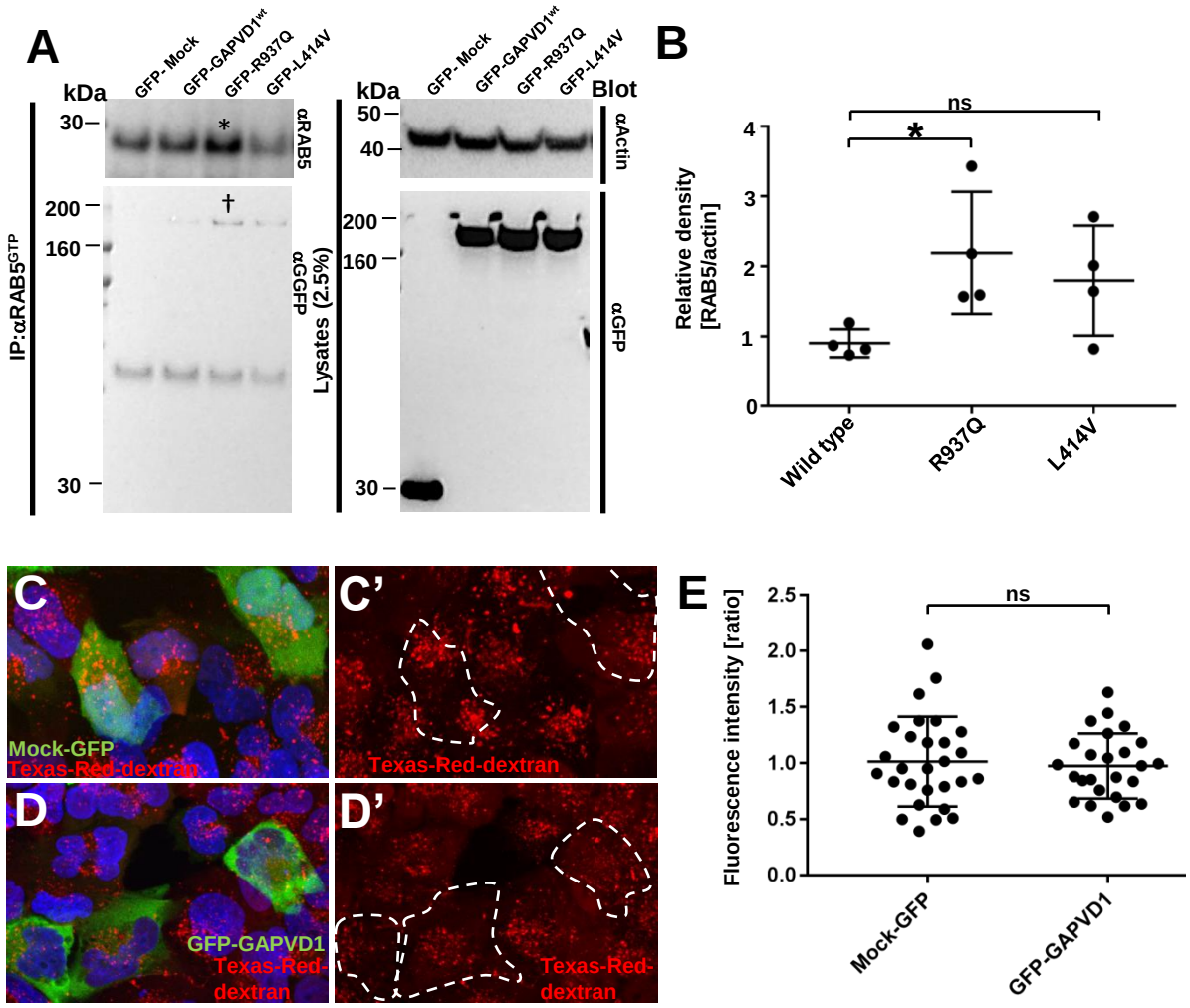

Supplementary Fig. 6. RAB5 activity assay and lack of an effect of *GAPVD1* overexpression on tracer endocytosis in human podocyte cell line.

(A) RAB5 activity assay in HEK293T cells. Cells express Mock-GFP, wild type GAPVD1 or GAPVD1 constructs that reflect the mutations that cause nephrotic syndrome. Compared to Mock-GFP, overexpressing wild type GAPVD1 does not result in a significant effect on RAB5 activity while the mutation from family B1381 (R937Q) increases active RAB5 (asterisk, see quantification in (B)). GFP staining reveals that compared to wild type GFP-GAPVD1 more GFP-GAPVD1-R937Q is precipitated along with the active RAB5 († sign). This suggests an increased affinity to active RAB5 compared to wild type.

(B) Quantitation of RAB5 activity shown as ratio of densities from RAB5 and actin normalized to Mock-GFP in experiments analogous to (A). The mutation R937Q significantly increases RAB5 activity while there is no significant effect of L414V. Each dot represents the result from one RAB5 assay normalized to an actin loading control (N=4).

(C-D') Human podocytes transfected with Mock-GFP (**C-C'**) or GFP-GAPVD1 (**D-D'**) were exposed to Texas-Red-dextran (10 kDa) for 30 min. Transfected cells do not differ from neighboring cells in the extent of Texas-Red-dextran-positive vesicles. For quantification see (E).

(E) Quantitation of fluorescence intensity of experiments from (A-B'). Values are expressed as a ratio to fluorescence intensity of neighboring untransfected cells. N=26 (GFP-GAPVD1) and N=28 (Mock) respectively.

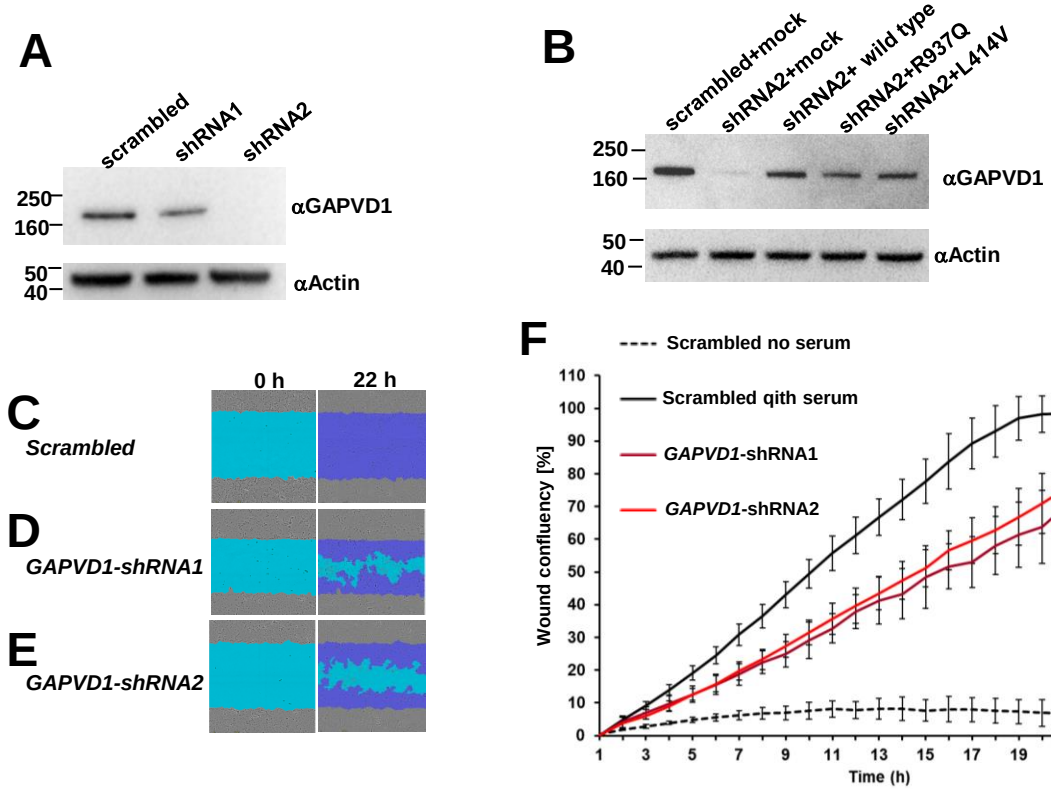

Supplementary Fig. 7. Characterization of stable shRNA lines used to measure podocyte migration rate for GAPVD1 (see Fig. 5A).

(A) Western blot from lysates of stable *GAPVD1*-shRNA or scrambled shRNA expressing human immortalized podocytes shows reduction of GAPVD1 by shRNA1 (weak knockdown) and *GAPVD1*-shRNA2 (strong knockdown).

(B) Western blot from lysates of stable *GAPVD1*-shRNA and scrambled shRNA expressing human immortalized podocytes co-transfected for rescue constructs. Scrambled shRNA and mock-rescue (GFP) confirm the strong reduction of shRNA2 (compare first to second lane). The wild type and mutant murine *Gapvd1* rescue constructs escape knockdown because shRNA is directed against human *GAPVD1* (lane three to five). The same is true for the murine *Gapvd1* cDNA harboring the respective loci of the mutations causing nephrotic syndrome(R937Q and L414, lanes four and five).

(C-E) Podocyte migration rate is analyzed by the IncuCyte videomicroscopy. Representative images show human podocytes directly after the scratch wound induction and 22 h thereafter. Scratch wound area (light blue) and podocytes that have migrated (dark blue) are shown. Representative images reveal wound confluency for podocytes expressing scrambled shRNA **(D),** while expression of two independent shRNA directed against *ANKFY1* gives rise to a strongly reduced podocyte migration and partial wound closure **(D** and **E)**.

(F) Graph shows wound confluence vs. time for the indicated genotypes. Error bars indicate SEM of 12 wells with identical conditions (18 wells per condition).

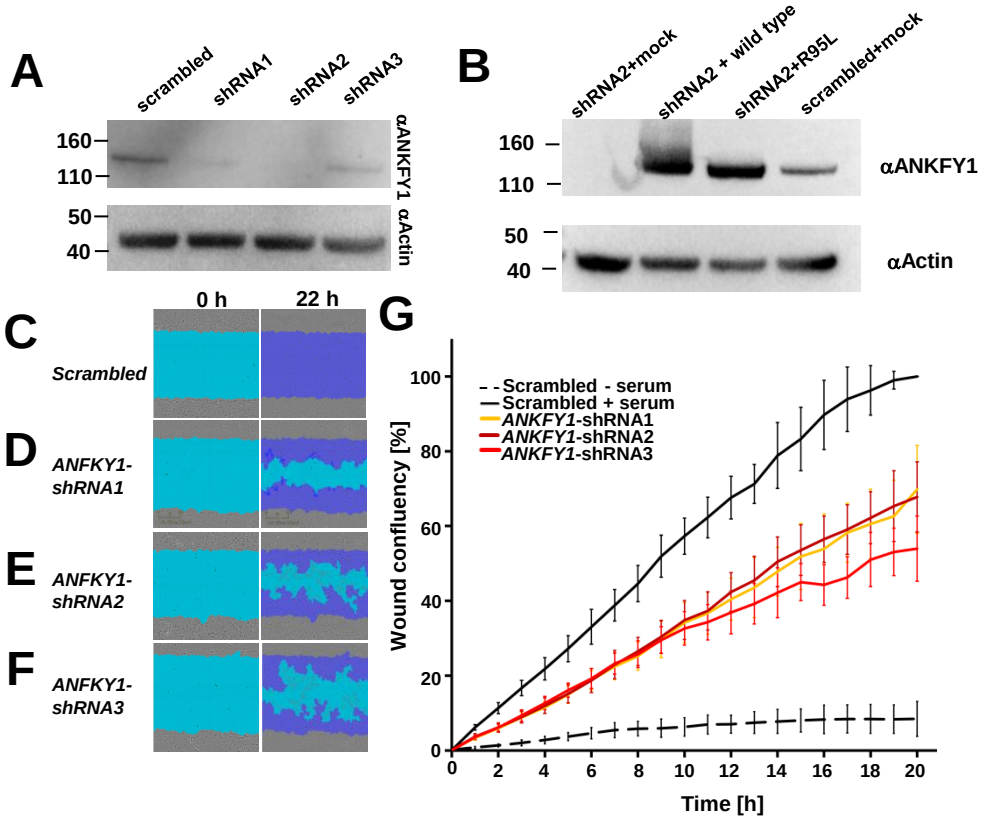

Supplementary Fig. 8. Characterization of stable shRNA lines used to measure podocyte migration rate for *ANKFY1* (see Fig. 5B).

(A) Western blot from lysates of stable *ANKFY1*-shRNA and scrambled shRNA expressing human immortalized podocytes. All three shRNAs tested resulted in knockdown of *ANKFY1*.

(B) Western blot from lysates of stable *ANKFY1*-shRNA and scrambled shRNA expressing human immortalized podocytes co-transfected for rescue constructs. Scrambled shRNA and mock-rescue (GFP) confirm the strong reduction of shRNA2 (compare first to second lane). The wild type and mutant *ANKFY1* rescue constructs escape knockdown because of synonymous mutations within the shRNA target sequence.

(C-F) Podocyte migration rate is analyzed by the IncuCyte videomicroscopy. Representative images show human podocytes directly after the scratch wound induction and 22 h thereafter. Scratch wound area (light blue) and podocytes that have migrated (dark blue) are shown. Representative images reveal wound confluency for podocytes expressing scrambled shRNA **(D),** while expression of two independent shRNA directed against *ANKFY1* gives rise to a strongly reduced podocyte migration and partial wound closure **(D-F)**.

(G) Graph shows wound confluence vs. time for the indicated genotypes. Error bars indicate SEM of 12 wells with identical conditions (18 wells per condition).

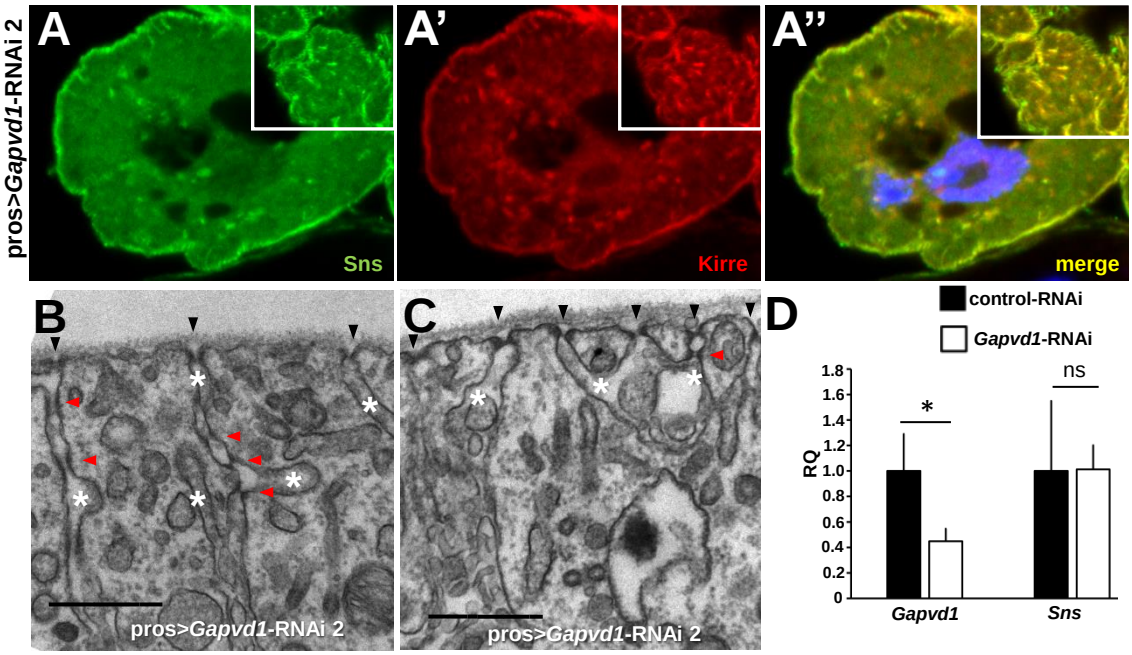

Supplementary Fig. 9. Phenotype of a second *Gapvd1-RNAi,* and qPCR analysis.

(A-A') Immunostaining of Sns and Kirre in *Drosophila* nephrocytes expressing *Gapvd1-RNAi2* reveals a thickening of the line of slit diaphragm proteins with protrusions towards the intracellular space and subcortical vesicular structures (inset shows subcortical section). (For comparison see control-RNAi **Fig. 6D-D''**, and *Gapvd1*-RNAi1 **Fig. 6E-E''**).

(B-C) Electron microscopy images of a nephrocyte expressing *Gapvd1*-RNAi2. The surface contains regular slit diaphragms but ectopic slit diaphragms are observed (red arrow head). Scale bar respresents 500 nm. (Control see **Fig. 6F**, *Gapvd1*-RNAi1 see **Fig. 6G-H**).

(D) qPCR from larvae expressing *Gapvd1*-RNAi1 ubiquitously with *actin-GAL4* using primers for *Gapvd1* and *sns.* The effect resulting from *RPL39* primers were used to normalize the results. The *Gapvd1* signal is reduced by *Gapvd1* knockdown while expression of *sns* appears unaffected.

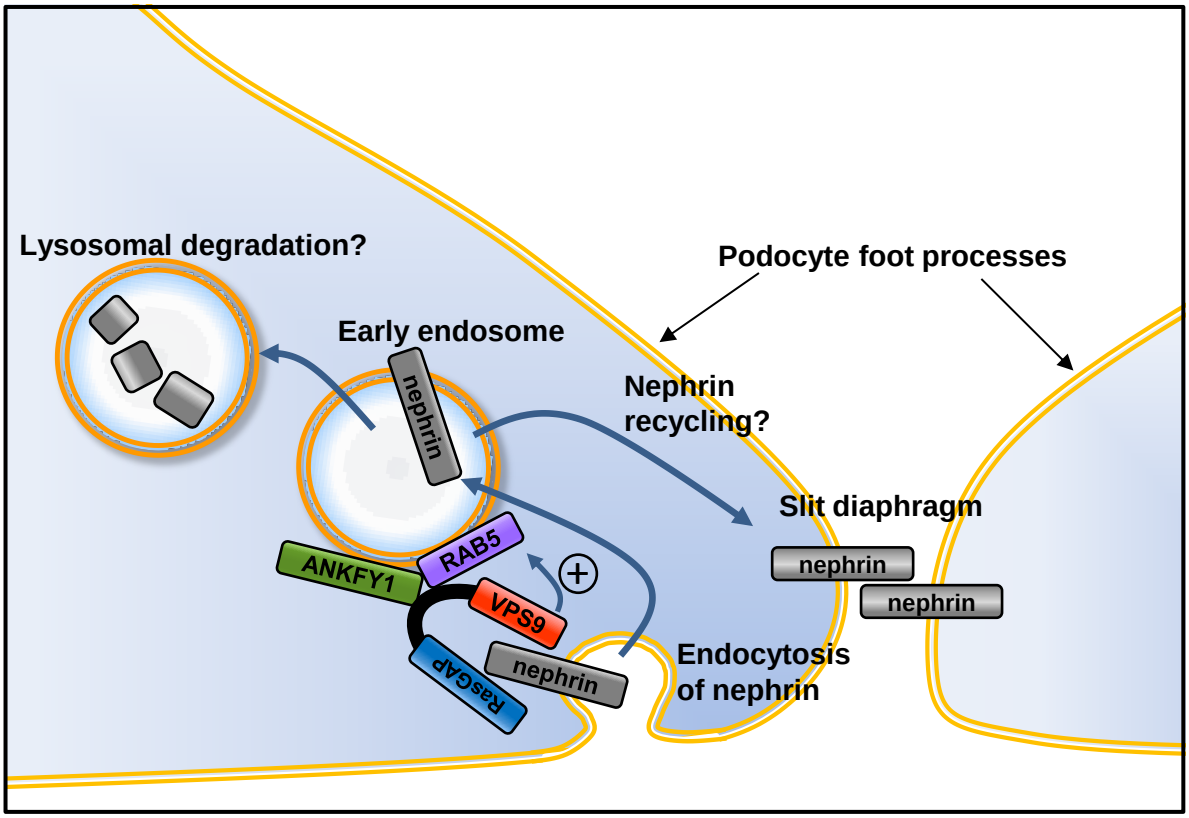

Supplementary Fig. 10. Hypothetical working model for GAPVD1 and ANKFY1 loss-of-function in podocytes.

Nephrin that is ectopically localized and not in a homodimer is subject to endocytosis upon binding to GAPVD1. Consecutive activation of RAB5 and ANKFY1 occurs, propagating removal of nephrin from the cell surface and further endosomal processing. This may either result in degradation or recycling of nephrin. In that way, endocytosis may serve to restrict nephrin to the slit diaphragm.

Supplementary Table 1: Primer sequences

Construct	Direction	Primer sequence
GAPVD1 full length human	forward	5'-ATGGTGAAACTAGATATTCATACTCTG
GAPVD1 full length human	reverse	5'-TCACTTTCGGTCATCGATGGTTTTA
GAPVD1- VPS9 domain human	forward	5'-ATACCAGAGGTTTATCTTCGAGAAG
GAPVD1- RasGAP domain	reverse	5'-CTATCAGGGAGTCATTTCTAAACTGCTACT
GAPVD1 VPS9 domain human	forward	5'-ATACCAGAGGTTTATCTTCGAGAAG
GAPVD1 full length mouse	forward	5'-ATGGTGAAGCTAGATATTCACACATTG
GAPVD1 full length mouse	reverse	5'-TCACTTTCTGTCATCGATGGTTTTAAT
GAPVD1 mutation R937Q	forward	5'-AGTGTCTTCTGTGCAGCGGCCCATGAGTG
mouse	reverse	5'-CACTCATGGGCCGCTGCACAGAAGACACT
GAPVD1 mutation L414V mouse	forward	5'-GTGGTGTATATAAGTTACAGTCAGGTTATTA CTCTGGTAAATTTTATGA
GAPVD1 mutation L414V mouse	reverse	5'-TCATAAAATTTACCAGAGTAATAACC TGACTGTAACTTATATACACCAC
GAPVD1 mutation R937Q human	forward	5'-TATAGTATCTTCTGTCCAG AGACCCATGAGTGACC
GAPVD1 mutation R937Q human	reverse	5'-GGTCACTCATGGGTCTCTGGACAGAAGATA CTATA
GAPVD1 mutation L414 human	forward	5'-CATAAAATTCACCAGAGTAATAACCTGACTGT AGGTTATATAAACCA
GAPVD1 mutation L414 human	reverse	5'-TGGTTTATATAACCTACAGTCAGGTTATTAC TCTGGTGAATTTTATG
GAPVD1 gRNA 1	forward	5'-CACCGTTGCTAACTGCTGCAAAAGG
GAPVD1 gRNA 1	reverse	5'-AAACCCTTTTGCAGCAGTTAGCAAC
GAPVD1 gRNA 2	forward	5'-CACCGGCGATCTGAAGATAAAGGTT
GAPVD1 gRNA 2	reverse	5'-AAACTCAGGTTTTGCGATACTTGAC
GAPVD1 shRNA 1	forward	5'-gatccGCCACTTTACATGAGCCAATTCGAAAA TTGGCTCATGTAAAGTGGCTTTTTTACGCGTg
GAPVD1 shRNA 2	reverse	5'-gatccGCACCTCATTCATCATCTTCACGAATGA AGATGATGAATGAGGTGCTTTTTTACGCGTg
ANKFY1 -ΔFYVE	reverse	5'-CTACTAGTTATTCACCCCGAGGCGAG
ANKFY1 mutation R95L human	forward	5'-GTCCTTCATCAGCCTTCTGCTGGCCATCG
ANKFY1 mutation R95L human	reverse	5'-CGATGGCCAGCAGAAGGCTGATGAAGGAC
ANKFY1 shRNA 1	forward	5'-gatccGCTGCCACTTTCCTCATTAAGCGAAC TTAATGAGGAAAGTGGCAGCTTTTTTACGCGTg
ANKFY1 shRNA 1	reverse	5'-aattcACGCGTAAAAAAGCTGCCACTTTCCTC ATTAAGTTCGCTTAATGAGGAAAGTGGCAGCg
ANKFY1 shRNA 2	forward	5'-gatccGCAGAAAGCCAATGCTCTTCACGAATG AAGAGCATTGGCTTTCTGCTTTTTTACGCGTg
ANKFY1 shRNA 2	reverse	5'-aattcACGCGTAAAAAAGCAGAAAGCCAATGCT CTTCATTCGTGAAGAGCATTGGCTTTCTGCg
ANKFY1 shRNA 3	forward	5'-gatccGCTCCTGGCATACATGAAAGGCGAAC CTTTCATGTATGCCAGGAGCTTTTTTACGCGTg
ANKFY1 shRNA 3	reverse	5'-aattcACGCGTAAAAAAGCTCCTGGCATACA TGAAAGGTTCGCCTTTCATGTATGCCAGGAGCg
ANKFY1 gRNA 1	forward	5'-CACCGTGGCAGCCCGCAGTGACAGC
ANKFY1 gRNA 1	reverse	5'-AAACGCTGTCACTGCGGGCTGCCAC
ANKFY1 gRNA 2	forward	5'-CACCGGCGATCTGAAGATAAAGGTT
ANKFY1 gRNA 2	reverse	5'-AAACAACCTTTATCTTCAGATCGCC
ANKFY1 shRNA resistant mutation	forward	5'-CCATTCTTAATGAGGAAGGTGGCGGCAAAG AGATCTCCTCT
ANKFY1 shRNA resistant mutation	reverse	5'-AGAGGAGATCTCTTTGCCGCCACCTTC CTCATTAAGAATGG
NPHS1 full length human	forward	5'-ATGGCCCTGGGGACGACG
NPHS1 full length human	reverse	5'-CTACACCAGATGTCCCCTCAGCT
NPHS1- R1160*	reverse	5'-CTAGGAATAAGACACCTCCTCCTG
NPHS1- aa1160-1241	forward	5'-CGAGGTTTCACAGGTGAAGATG
NPHS1 -aa1084-1160	forward	5'-CTCTGGCAGCGGAGACTCA